

*Citation for published version:*

Mosley, PJ, Bateman, SA, Lavoute, L & Wadsworth, WJ 2011, 'Low-noise, high-brightness, tunable source of picosecond pulsed light in the near-infrared and visible', *Optics Express*, vol. 19, no. 25, pp. 25337-25345.  
<https://doi.org/10.1364/OE.19.025337>

*DOI:*

[10.1364/OE.19.025337](https://doi.org/10.1364/OE.19.025337)

*Publication date:*

2011

[Link to publication](#)

This paper was published in Optics Express and is made available as an electronic reprint with the permission of OSA. The paper can be found at the following URL on the OSA website: [article URL]. Systematic or multiple reproduction or distribution to multiple locations via electronic or other means is prohibited and is subject to penalties under law.

## University of Bath

### Alternative formats

If you require this document in an alternative format, please contact:  
[openaccess@bath.ac.uk](mailto:openaccess@bath.ac.uk)

#### General rights

Copyright and moral rights for the publications made accessible in the public portal are retained by the authors and/or other copyright owners and it is a condition of accessing publications that users recognise and abide by the legal requirements associated with these rights.

#### Take down policy

If you believe that this document breaches copyright please contact us providing details, and we will remove access to the work immediately and investigate your claim.

# Low-noise, high-brightness, tunable source of picosecond pulsed light in the near-infrared and visible

Peter J. Mosley,\* Samuel A. Bateman, Laure Lavoute,  
and William J. Wadsworth

*Centre for Photonics and Photonic Materials, University of Bath, Bath, BA2 7AY, UK*

*\*[pjm36@bath.ac.uk](mailto:pjm36@bath.ac.uk)*

**Abstract:** We have built a flexible source of picosecond pulsed light in both the near-infrared and visible spectral regions. A photonic crystal fiber (PCF) was pumped with a pulsed 1064 nm fiber laser to generate four-wave mixing (FWM) sidebands at 947 nm and 1213 nm. This process was seeded at the idler wavelength with a tunable diode laser to limit the spectral width of the sidebands to less than 0.5 nm. Subsequently the idler was mixed efficiently with the residual pump in a nonlinear crystal to yield their sum frequency at 567 nm. All three outputs were tunable by adjusting the seed wavelength and all had very low pulse-to-pulse amplitude noise. This technique could be extended to different wavelength ranges by selecting different seed lasers and PCF.

© 2011 Optical Society of America

**OCIS codes:** (190.4380) Nonlinear optics, four-wave mixing, (190.4970) Parametric oscillators and amplifiers, (060.5295) Photonic crystal fibers.

---

## References and links

1. J. M. Dudley and J. R. Taylor, "Ten years of nonlinear optics in photonic crystal fibre," *Nat. Photonics* **3**(2), 85–90 (2009). URL <http://dx.doi.org/10.1038/nphoton.2008.285>.
2. J. M. Dudley, G. Genty, and S. Coen, "Supercontinuum generation in photonic crystal fiber," *Rev. Mod. Phys.* **78**(4), 1135 (2006). URL <http://link.aps.org/abstract/RMP/v78/p1135>.
3. Q. Li, F. Li, K. K. Y. Wong, A. P. T. Lau, K. K. Tsia, and P. K. A. Wai, "Investigating the influence of a weak continuous-wave-trigger on picosecond supercontinuum generation," *Opt. Express* **19**(15) 757–1769 (2011). URL <http://www.opticsexpress.org/abstract.cfm?URI=oe-19-15-13757>.
4. L. E. Hooper, P. J. Mosley, A. C. Muir, W. J. Wadsworth, and J. C. Knight, "Coherent supercontinuum generation in photonic crystal fiber with all-normal group velocity dispersion," *Opt. Express* **19**(6), 4902–4907 (2011). URL <http://www.opticsexpress.org/abstract.cfm?URI=oe-19-6-4902>.
5. M. H. Dunn and M. Ebrahimzadeh, "Parametric Generation of Tunable Light from Continuous-Wave to Femtosecond Pulses," *Science* **286** (5444), 1513–1517 (1999).
6. G. Cerullo and S. D. Silvestri, "Ultrafast optical parametric amplifiers," *Rev. Sci. Instrum.* **74**(1), 1–18 (2003). URL <http://link.aip.org/link/?RSI/74/1/1>.
7. J. E. Sharping, M. Fiorentino, A. Coker, P. Kumar, and R. S. Windeler, "Four-wave mixing in microstructure fiber," *Opt. Lett.* **26**(14), 1048–1050 (2001). URL <http://ol.osa.org/abstract.cfm?URI=ol-26-14-1048>.
8. K. Inoue, "Suppression of level fluctuation without extinction ratio degradation based on output saturation in higher order optical parametric interaction in fiber," *IEEE Photon. Tech. Lett.* **13**(4), 338–340 (2001).
9. P. Kylemark, P. Hedekvist, H. Sunnerud, M. Karlsson, and P. Andrekson, "Noise characteristics of fiber optical parametric amplifiers," *J. Lightwave Technol.* **22**(2), 409–416 (2004).
10. W. Wadsworth, N. Joly, J. Knight, T. Birks, F. Biancalana, and P. Russell, "Supercontinuum and four-wave mixing with Q-switched pulses in endlessly single-mode photonic crystal fibres," *Opt. Express* **12**(2), 299–309 (2004). URL <http://www.opticsexpress.org/abstract.cfm?URI=oe-12-2-299>.

11. A. Y. H. Chen, G. K. L. Wong, S. G. Murdoch, R. Leonhardt, J. D. Harvey, J. C. Knight, W. J. Wadsworth, and P. S. J. Russell, "Widely tunable optical parametric generation in a photonic crystal fiber," *Opt. Lett.* **30**(7), 762–764 (2005). URL <http://ol.osa.org/abstract.cfm?URI=ol-30-7-762>.
12. C. Xiong, A. Witkowska, S. G. Leon-Saval, T. A. Birks, and W. J. Wadsworth, "Enhanced visible continuum generation from a microchip 1064nm laser," *Opt. Express* **14**(13), 6188–6193 (2006). URL <http://www.opticsexpress.org/abstract.cfm?URI=oe-14-13-6188>.
13. T. Sloanes, K. McEwan, B. Lowans, and L. Michaille, "Optimisation of high average power optical parametric generation using a photonic crystal fiber," *Opt. Express* **16**(24), 19,724–19,733 (2008). URL <http://www.opticsexpress.org/abstract.cfm?URI=oe-16-24-19724>.
14. D. Nodop, C. Jauregui, D. Schimpf, J. Limpert, and A. Tünnermann, "Efficient high-power generation of visible and mid-infrared light by degenerate four-wave-mixing in a large-mode-area photonic-crystal fiber," *Opt. Lett.* **34**(22), 3499–3501 (2009). URL <http://ol.osa.org/abstract.cfm?URI=ol-34-22-3499>.
15. L. Lavoute, J. C. Knight, P. Dupriez, and W. J. Wadsworth, "High power red and near-IR generation using four wave mixing in all integrated fibre laser systems," *Opt. Express* **18**(15), 16,193–16,205 (2010). URL <http://www.opticsexpress.org/abstract.cfm?URI=oe-18-15-16193>.
16. J. Hansryd, P. Andrekson, M. Westlund, J. Li, and P.-O. Hedekvist, "Fiber-based optical parametric amplifiers and their applications," *IEEE J. Sel. Top. Quantum Electron.* **8**(3), 506–520 (2002).
17. C. J. McKinstrie and M. G. Raymer, "Four-wave-mixing cascades near the zero-dispersion frequency," *Opt. Express* **14**(21), 9600–9610 (2006). URL <http://www.opticsexpress.org/abstract.cfm?URI=oe-14-21-9600>.

## 1. Introduction

Supercontinuum generation in photonic crystal fiber (PCF) has been phenomenally successful over the past decade in extending the spectral reach of laser light sources [1]. It is remarkable that by propagating high-intensity pulses centered at 800 nm or 1064 nm with only modest pulse energy through a few metres of PCF one can obtain a spectrum spanning from the edge of the ultraviolet to the mid-infra-red. Due to their many favourable characteristics (emission into a single spatial mode, versatility, low cost, and ease of use) these light sources have proved their worth in a host of applications, however they are not always ideal. The input pulse energy is spread over such a wide wavelength range that the spectral power density is usually quite low (on the order of 1mW/nm from a 20 MHz system); hence if a narrow wavelength range is filtered from the supercontinuum, the mean power will be small. Furthermore, because the spectral broadening is typically dependent on highly-nonlinear soliton-based processes, the output consists of multiple sub-pulses and exhibits a high level of noise. This noise is manifest in pulse-to-pulse fluctuations not only of the spectral amplitude but also of the arrival times of individual sub-pulses [2]. Seeding the supercontinuum can result in a moderate reduction in this noise [3], or it can be eliminated entirely by using an all-normal-dispersion PCF at the expense of significantly reduced bandwidth [4].

Parametric generation techniques in bulk optics have long been used for producing wavelengths that are not accessible directly using conventional lasers [5]. However, the ability of these sources to produce high powers over a broad range of wavelengths comes at a high price in terms of the complexity and cost of the optics required [6]. We have been focussing on developing light sources based on four-wave-mixing (FWM) in PCF [7]. For a wide range of wavelengths, FWM has the capability to address the problems of low power density inherent in the majority of supercontinuum sources while retaining the desirable characteristics of good spatial mode quality, low cost, and ease of use [8–11]. However, it is difficult to limit the bandwidth of the generated light to less than a few nm at best and also to obtain good conversion efficiencies into spectral regions far from the pump (for example to wavelengths of less than 650 nm for a pump at 1064 nm) [12–15].

Here we present a source of narrowband, tunable, picosecond pulses of light in a single spatial mode in both the near-infrared and visible spectral regions. Using a PCF, we generated narrow FWM sidebands in the near-infrared by parametric amplification [16] of a continuous-wave (CW) seed by a 0.5 MHz amplified fiber laser at 1064 nm. Both FWM sidebands had

bandwidths of less than 0.5 nm (much narrower than previous PCF-based FWM light sources [10, 11, 13, 15]) and average spectral power densities in excess of 30 mW/nm; they were tunable between 910–950 nm (signal) and 1210–1280 nm (idler) by changing the seed wavelength.

The use of a narrowband seed resulted in high quality output pulses in both the spectral and temporal domains, allowing us subsequently to carry out sum-frequency generation (SFG) in a  $\chi^{(2)}$  nonlinear crystal. We converted the residual pump and FWM idler to a 0.1 nm full-width at half-maximum (FWHM) band that could be tuned from 567 nm to 581 nm. This had a spectral power density of approximately 20 mW/nm and the maximum conversion efficiency from 1064 nm was over 2%. Furthermore, we show that conversion to any of these spectral bands was possible with no measurable increase in noise over that of the pump. These techniques are applicable to other wavelength ranges by selecting different lasers and PCF.

## 2. Experiment

The FWM PCF used in the experiments reported here was fabricated at the University of Bath. It was made from silica glass using the stack-and-draw process to obtain a pitch (hole spacing,  $\Lambda$ ) of 3.1  $\mu\text{m}$  and a hole diameter to pitch ratio ( $d/\Lambda$ ) of 0.31. Two opposing holes adjacent to the core were made larger than the others in the cladding by including in the stack two capillaries with larger holes. In the drawn fiber these holes were 1.5 times the diameter of the remaining holes in the cladding structure thus making it birefringent.

The experimental apparatus is shown in Fig. 1. Our FWM pump laser was an amplified, modelocked 1064 nm fiber laser from Fianium Ltd., pulse-picked to operate at 0.5 MHz. The average output power was 200 mW, the pulse duration was approximately 40 ps, and the FWHM spectral bandwidth was  $\sim 0.25$  nm. A half-wave plate (HWP) and polarizing beamsplitter (PBS) were used to control the pump power, and the rejected beam from the PBS was directed to a fast InGaAs photodiode (InGaAs PD) to monitor the pump pulses. The transmitted beam from the PBS was reflected from a long-wave-pass dichroic mirror (DM) and coupled into the FWM PCF with an efficiency of a little over 50%, giving a peak power in the fiber of approximately 5 kW. The seed laser was a home-built CW external-cavity tunable diode laser (TDL), based on the SAF1175S fiber-coupled half-butterfly gain chip available from Thorlabs. The average power of this laser was 50 mW at its central wavelength of 1220 nm and it could be tuned over a range of more than  $\pm 50$  nm. It had a FWHM bandwidth of less than 0.1 nm. The single-spatial-mode output from the fiber pigtail was directed through the DM and coupled into the FWM fiber concurrently with the pump laser, also with an efficiency of 50%. The pump and the seed were set independently to have the same linear polarization; this was oriented along one axis of the PCF using a HWP common to both beams.

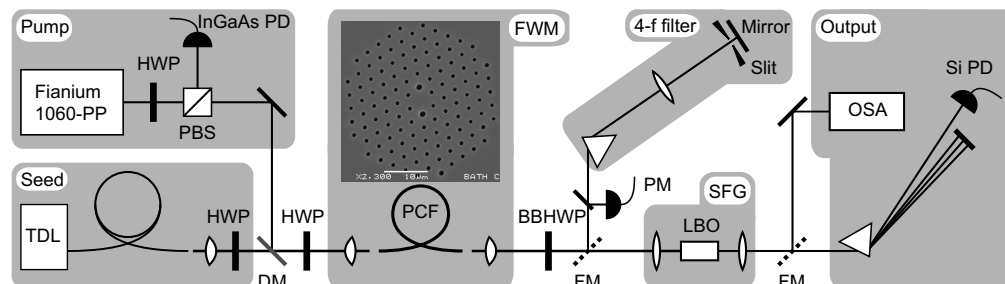


Fig. 1. Apparatus and scanning electron micrograph of PCF end face. See text for details.

The output from the FWM PCF passed through a broadband HWP (BBHWP) specified to operate between 690 nm and 1200 nm and could be directed either via a flipper mirror (FM) to a

4-f prism filter or directly to the sum frequency apparatus. The central transmission wavelength of the prism filter could be varied across the entire FWM spectrum (from below 900 nm to above 1300 nm) and its bandwidth could be adjusted as required. In this configuration the HWP following the PCF was used to set the polarization of the FWM to be horizontal, giving the filter a mean in-band transmission of 0.65. The output of the filter could be directed to a power meter (PM). In order to perform SFG, the polarization of the entire FWM output was rotated to be vertical and it was focused using a 75 mm focal length lens into a 15 mm long noncritically-phasematched lithium triborate (LBO) crystal. The crystal was housed in an oven to allow temperature tuning between room temperature and 200°C. The crystal output was collimated and could be dispersed by a single prism to allow observations by eye and measurements of the sum-frequency (SF) component free from the residual FWM. Type-I phasematching in the LBO crystal ensured that the SF light was horizontally polarized and therefore approximately Brewster-angled upon arrival at the prism so little power was lost. The SF component was monitored either with a power meter or a fast silicon photodiode (Si PD) as shown. Alternatively the entire beam after the LBO crystal could be coupled into a multimode fiber and the full spectrum (of the residual pump, the FWM, and the SF) recorded on an optical spectrum analyzer (OSA, Ando AQ6315B).

Pump and seed powers are expressed as the average power propagating in the PCF, measured at the output end of the PCF. All the experiments reported here were performed using the same 390 mm length of PCF, chosen for optimum SF efficiency with 100 mW of pump power. For shorter fibers, the SF power was reduced as the FWM was less efficient, whereas for longer fibers the SF power was reduced due to nonlinear broadening of the pump and the generated FWM.

### 3. Four-wave mixing in the near-infrared

Pumping our PCF at 1064 nm without seeding we observed low-intensity, broadband spontaneous FWM. The effects of the fiber's birefringence upon the phasematching were clear when switching the pump between the two principal axes, as shown in Fig. 2(a). Pumping on one fiber axis the peak signal (idler) gain was at approximately 930 nm (1240 nm) while on the other axis the peak gain occurred at 900 nm (1290 nm), suggesting that the zero-dispersion wavelength was at approximately 1068 nm. In both cases the FWM was generated with the same polarization as the pump. The spontaneous FWM was approximately 30 dB lower in intensity than the pump and the signal and idler FWHM bandwidths were 20 nm and 40 nm respectively.

The radical effect of seeding at the idler wavelength can be seen in Fig. 2(b). Seeding at a wavelength of 1213 nm reduced the FWM bandwidths by almost two orders of magnitude, yielding a narrow-band conjugate at 947 nm. The narrow peaks at 777 nm, 853 nm, and 1411 nm in Fig. 2(b) are cascaded FWM processes [17] and the broad peak at 1030 nm is CW amplified spontaneous emission (ASE) from the pump laser; this also seeds a poorly-phasematched FWM process to generate weak (pulsed) light at 1100 nm. High-resolution plots of the seeded FWM peaks are shown in Fig. 2(d) and (f). The seeded FWM signal had a FWHM bandwidth of 0.37 nm and the idler bandwidth was 0.32 nm. As shown in Fig. 2(f), the generated idler spectrum was estimated by finding the difference between the seeded FWM spectrum at 1213 nm and the spectrum with only the seed present in the PCF. This is a valid approximation as, due to the mark-space ratio of the pump laser, the fraction of the CW seed involved in the FWM interaction was only around  $2 \times 10^{-5}$  of the total. The maximum power generated in the signal was 15.8 mW (measured after the 4-f filter and corrected for filter loss) corresponding to a conversion efficiency from coupled pump power of over 15%. As the repetition rate was only 0.5 MHz this gives a pulse energy for the signal of over 30 nJ. It is reasonable to assume that the pulse duration of the signal was similar to that of the pump as the fiber length was much

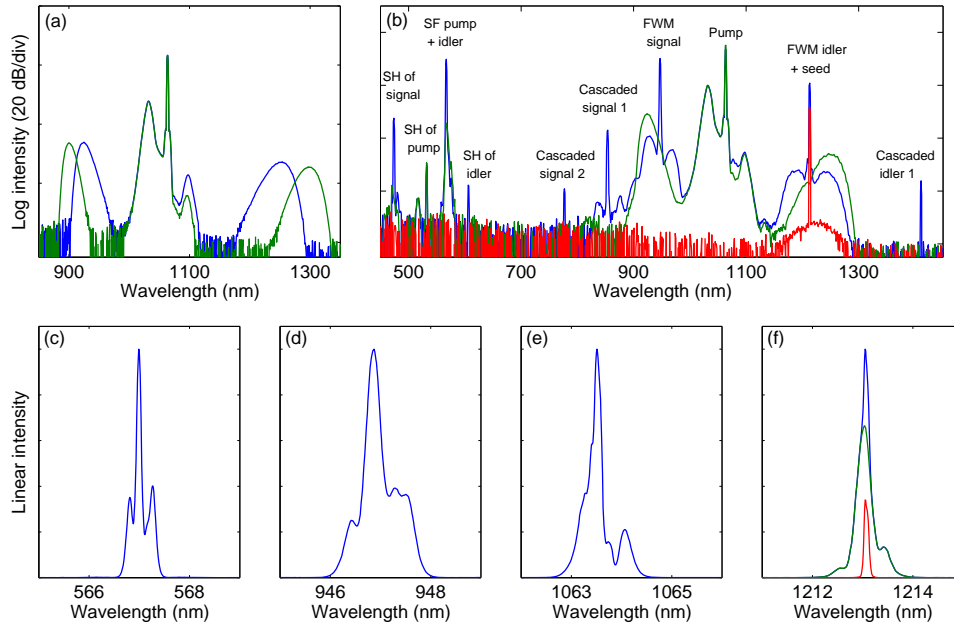


Fig. 2. Spectra from a 390 mm length of FWM PCF with a pump power of 105 mW. (a) Spontaneous FWM (seed laser off) for each fiber axis, measured directly after the PCF. (b) Seeded FWM and SFG measured after the LBO crystal. Seed power of 1.1 mW (blue), unseeded (green), and seed only with pump blocked (red). Lower row shows individually normalized high-resolution (0.05 nm) spectra of each line also at a seed power of 1.1 mW, plotted on a linear scale: (c) SF; (d) FWM signal; (e) pump; (f) FWM idler as recorded (blue), seed only (red), idler minus seed (green).

less than the walkoff length (approximately 20 m for pump and signal), hence the peak power of the signal can be estimated to have been approximately 750 W. Figures were similar for the idler.

We calculated the maximum FWM gain at the idler wavelength by operating around the seeding threshold. For a seed power of  $36 \mu\text{W}$ , at the maximum pump power the FWM idler output was measured to be 2.2 mW after propagation through 390 mm of PCF (the corresponding power in the unseeded idler was 0.41 mW). When seeded, the ratio of input to output power was 61, and hence the time-averaged gain at the seed wavelength was 18 dB. However, taking the mark-space ratio of the pump to define the fraction of the CW seed that actually takes part in the FWM interaction, the resulting amplification factor for this part of the seed is  $3.0 \times 10^6$ , yielding a FWM gain of 65 dB.

#### 4. Sum-frequency generation of visible pulses

The change resulting from seeding is even more dramatic in the SF output, shown in Figs. 2(b) and (c). Without seeding there was negligible SF generated (less than 0.1 mW), due both to the low power and broad bandwidth of the FWM idler (the majority of which could not be simultaneously phasematched in the long LBO crystal). However, when the idler was reduced in bandwidth and increased in power by coupling the seed into the PCF, the SF beam appeared bright to the naked eye and its FWHM bandwidth was reduced commensurately to 0.11 nm. In the optimum configuration, it had an average power of over 2 mW, corresponding to a pulse energy



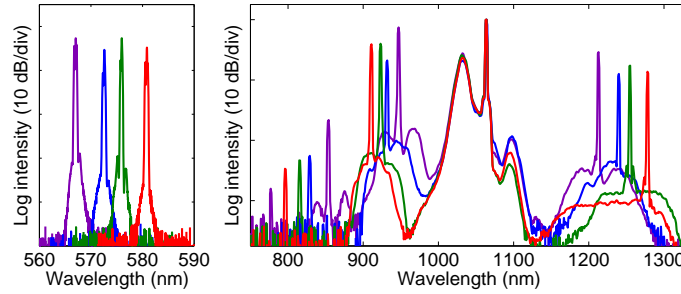


Fig. 3. Seed tuning. Seed wavelengths of 1213 nm (purple), 1240 nm (blue), 1255 nm (green), and 1278 nm (red). Pump power 100 mW, seed power in the range 1–10 mW.

of 4 nJ and representing an efficiency from coupled pump power to SF of approximately 2 %. In this case, the SF was at 567 nm and additionally there were three poorly-phasematched second harmonic (SH) peaks near the SF: 607 nm (SH of 1213 nm idler), 532 nm (SH of 1064 nm pump; this appears also in the unseeded case), and 474 nm (SH of 947 nm signal). The intensity of all the SH components was very low; it could be increased for each one individually by temperature-tuning the LBO crystal but (with the exception of 532 nm) the power in each SH component was never more than  $100 \mu\text{W}$ . Using a fast photodiode and sampling oscilloscope, the SF was observed to consist of a single pulse in the time domain with a duration of less than 40 ps (limited by the measurement bandwidth).

## 5. Optimization and noise measurements

The tuning capability of our source is demonstrated in Fig. 3. By tuning the seed from 1213 nm to 1278 nm the FWM signal was tuned from 947 nm to 911 nm and the SF from 567 nm to 581 nm respectively. This was achieved at almost constant SF power due to the flexibility afforded by the different phasematching conditions of the two fiber axes: the spectra with the seed at 1213 nm and 1240 nm (SF at 567 nm and 573 nm) were obtained using one axis, and the spectra with the seed at 1255 nm and 1278 nm (SF at 576 nm and 581 nm) with the other axis. As a result of the noncritical phasematching of the SFG crystal, only its temperature (and not its angle) needed to be adjusted to ensure proper phasematching each time the seed wavelength was changed. Furthermore, noncritical phasematching allowed the exceptionally high beam quality of the fiber mode to be replicated in the SF as the light propagated along one of the crystal's optic axes without spatial walkoff.

Figure 4 shows the dependence of both the FWM signal and the SF output powers on seed power and pump power. The signal power was measured by switching the PCF output into the prism filter and selecting only the signal wavelength. Note that, in order to take account of the filter transmission of 0.84, the plotted signal powers must be multiplied by  $\sim 1.2$  to obtain the signal power directly after the PCF.

The seed power was varied from zero up to the maximum available power of 32 mW at a pump power of approximately 100 mW. As the plot in Fig. 4(a) demonstrates, the threshold for seeding was very low (around  $30 \mu\text{W}$ ). Above threshold the signal and SF power increased rapidly. The signal power peaked at a seed power of 4 mW – due to the mark-space ratio of the pump laser, this corresponds to an average power of only 80 nW interacting with the pump pulses. At higher seed powers, the signal power fell due to increased nonlinear conversion into wavelengths not transmitted by the filter. The SF power gradually rose as the seed was increased towards its maximum power.

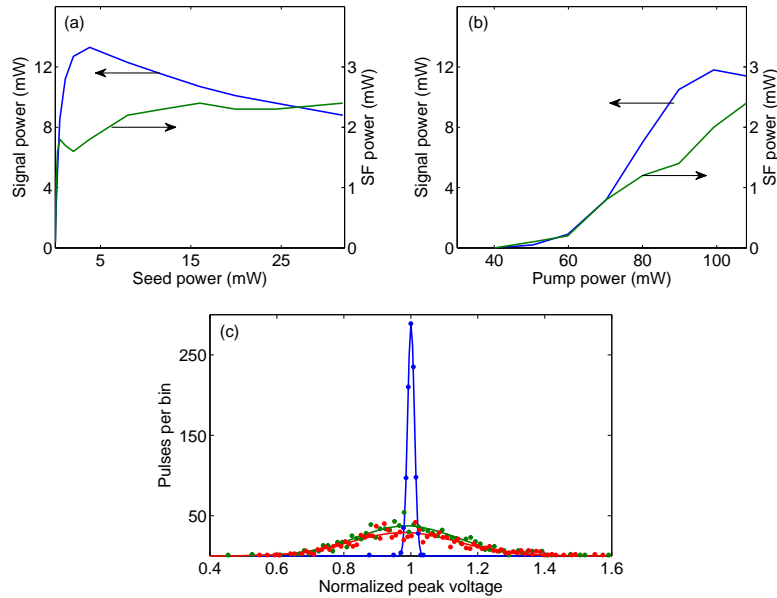


Fig. 4. (a) Output power as a function of seed power and (b) of pump power. (c) Distributions of pulse energy in 1000 pulses of seeded FWM SF (blue), unseeded FWM SF (green), and filtered supercontinuum (red). Lines are least-square Gaussian fits.

The dependence on pump power was investigated with the seed power fixed at 10 mW. From Fig. 4(b) we can see that, once over the FWM pump threshold at 40 mW, the increase in signal power was initially quadratic with pump power but then slowed down towards 100 mW. This roll-off occurred due to the broadening of the pump by the fiber nonlinearity, and also because the fiber length was chosen for a pump power of 100 mW to be optimal for SFG rather than FWM. However, the SF power, due to its dependence on both the pump power and the signal power, does not show the same trend. The SF power increases approximately linearly from the FWM threshold to the maximum available power and it appears that if we could increase our pump power beyond 108 mW the SF power would continue to increase.

For a fixed seed power, the bandwidths of both the FWM and SF changed slightly with both pump power and seed wavelength. However, for the range of pump powers used here, the seed power could always be adjusted to minimize the bandwidths and give values similar to those listed above. Typically the seed power required was between 1–10 mW and after this adjustment had been made the output powers were close to their maxima, as suggested by Fig. 4(a).

We carried out noise analysis using four photodiodes, two of which are shown in Fig. 1. Si photodiodes were used to measure the signal and SF pulses; InGaAs photodiodes monitored the idler and the pump (to ensure that its noise remained constant throughout). A digital oscilloscope connected to a PC was used to record the maximum voltage registered by each photodiode for each of 1000 trigger events (each trigger corresponded to a single optical pulse). The response time of the photodiodes was slow compared to the pulse duration and hence these maximum voltages were proportional to the pulse energy. Measurements were first performed for seeded FWM and SF, and then for spontaneous FWM and SF with the seed laser blocked. Subsequently, the FWM PCF was replaced with a 7 m length of highly-nonlinear PCF in which the pump propagated in the anomalous dispersion regime, generating a supercontinuum spanning the visible. A 35 nm bandwidth section centered at 570 nm was filtered from this



supercontinuum using the prism filter, and the noise measurement was repeated for 1000 pulses of the supercontinuum. A relatively broad wavelength range had to be used to obtain enough signal from the photodiode due to the low spectral power density of the supercontinuum.

Table 1. Measured noise figures, expressed as standard deviations of Gaussian fits to normalized pulse energy distribution data (similar to that shown in Fig. 4(c)). Errors are 95% confidence bounds on the standard deviations of the fits. Note that in the seeded case, the signal and idler data were taken at a seed power of 12 mW and the SF at a seed power of 1 mW. Pump power was approximately 100 mW throughout.

	Pump	Signal	Idler	SF	SC
Unseeded	0.012(1)	0.21(2)	0.19(2)	0.17(1)	0.16(1)
Seeded		0.0065(2)	0.0060(1)	0.0096(1)	

Examples of normalized pulse energy histogram data are displayed in Fig. 4(c) along with Gaussian fits to the distributions, and the noise figures are shown in Table 1. It is clear that the unseeded FWM, unseeded SF, and the supercontinuum (SC) were very noisy, with fractional standard deviations in pulse energy of 15–20%. The high noise level in spontaneous FWM is because the generated fields are initiated by quantum zero-point fluctuations which are inherently random. The supercontinuum is a result of spectral broadening that is also seeded from noise and depends on soliton effects that are very sensitive to the initial pump pulse conditions, greatly amplifying any noise that is already present [2].

In contrast, when the FWM process was seeded, the amplitude noise was drastically reduced. The seeded FWM signal and idler as well as the SF had very low amplitude noise, all exhibiting fractional standard deviations in their pulse energy of less than 1%. These measurements demonstrate explicitly one of the primary advantages of seeded FWM: the signal and idler (as well as subsequent nonlinear interactions) can be incredibly stable with no increase in pulse-to-pulse amplitude noise over that of the pump laser.

## 6. Conclusion

Using a 1064 nm amplified fiber laser pulsed at 0.5 MHz, we have demonstrated the generation of narrowband tunable picosecond pulses between 910–950 nm and 1210–1280 nm by seeded FWM in a PCF and between 567 nm–581 nm by subsequent SFG of the FWM idler and residual pump. The beam quality of all outputs was very high due to the use of a single-mode PCF and noncritically-phasematched nonlinear crystal. The peak power in both near-infrared pulses was approximately 750 W, their spectral power density was over 30 mW/nm, and the generation efficiency of each was about 15 %. The visible pulses had a peak power of approximately 100 W, spectral power density around 20 mW/nm, and an overall generation efficiency (taking into account both cascaded nonlinear processes) of over 2 %. The amplitude noise of all three outputs was limited only by that of the pump, and each consisted of a single pulse in the time domain. Scaling this up to a 20 MHz laser system with the same pulse parameters as our 0.5 MHz system (possible with current technology as it requires an average power of only 8 W) would yield pulses with a spectral power density of 800 mW/nm in the visible and 1.2 W/nm in the IR.

This technique can be readily extended to other wavelengths. For example, by using a seed laser similar to the one reported here but emitting at 1375 nm, coupled to a slightly different PCF, one could generate SF pulses at 600 nm. Furthermore, by seeding at 1550 nm the FWM signal would fall in the middle of the Ti:Sapphire wavelength range, at 810 nm.

## **Acknowledgments**

This work was supported by the UK Technology Strategy Board. We thank T. A. Birks for helpful comments on the manuscript.